Electronic Supplementary Material (ESI) for Environmental Science: Nano.
This journal is © The Royal Society of Chemistry 2022

Supporting Information

Interaction of pyrite with zerovalent iron with superior reductive ability via Fe(II) regeneration

Qi Li [a], Zhi Jiang [a], Junhao Zheng [a], Yan Xie [a], Qi Liao [a, b], Feiping Zhao [a, b], Zhihui Yang [a, b], Zhang Lin [a, b, c], Mengying Si [a, b *], Weichun Yang [a, b *]

[a] School of Metallurgy and Environment, Central South University, Changsha 410083, P.R. China

[b] Chinese National Engineering Research Centre for Control & Treatment of Heavy Metal Pollution, Changsha 410083, P.R. China

[c] School of Environment & Energy, South China University of Technology, Guangzhou 510006, P.R. China

* Corresponding author:

Mengying Si, E-mail address: simysmile@csu.edu.cn

Weichun Yang, E-mail address: yang220@csu.edu.cn

32 Pages, 23 Figures, and 4 Tables

CONTENTS

Fig. S15. (a) Cr(VI) removal by mixed FeS_2-ZVI and FeS_2/ZVI in the absence or presence of 1,10-phenanthroline.

Fig. S16. Dissolution of Fe from mixed FeS_2-ZVI and FeS_2/ZVI in pure water system.

Fig. S17. Effect of different amount of Fe^{2+} added on Cr(VI) removal.

Fig. S18. XRD patterns of FeS_2/ZVI, FeS/ZVI and S/ZVI.

Fig. S19. Lattice constants of Fe BCC structure according to XRD Rietveld refinement.

Fig. S20. Water contact angle images of FeS_2/ZVI, FeS/ZVI, and S/ZVI.

Fig. S21. The influence of S precursors on hydrophobicity and Cr(VI) removal.

Fig. S22. The reusability of FeS_2/ZVI at initial pH 5.20 for Cr(VI) removal and rejuvenation of FeS_2/ZVI by BM again.

Fig. S23. Image of the magnetic separation after the Cr(VI) removal by FeS_2/ZVI.

Table S1. The ^{57}Fe Mossbauer parameters[a] of FeS_2/ZVI.

Table S2. Removal rate of Cr(VI) by FeS_2/ZVI at different pyrite to zero-valent iron molar ratio.

Table S3. Linear regression analysis of mixed FeS_2-ZVI and FeS_2/ZVI for the kinetics of Cr(VI) removal.

Table S4. Intrinsic properties of FeS_2/ZVI (molar ratio 9:1).

Cr(VI) removal kinetics

Pseudo first-order model：

$$\frac{dQ_t}{dt} = k_1(Q_e - Q_t) \tag{1}$$

$$\ln (Q_e - Q_t) = \ln Q_e - k_1 t \tag{2}$$

Pseudo second-order model：

$$\frac{dQ_t}{dt} = k_2(Q_e - Q_t)^2 \tag{3}$$

$$\frac{t}{Q_t} = \frac{1}{k_2 {Q_e}^2} + \frac{1}{Q_e}t \tag{4}$$

where k is the rate constant of Cr(VI) removal by mixed FeS_2-ZVI and ball milled FeS_2/ZVI, Q_e is the amount of adsorbate at equilibrium (mg g^{-1}); Q_t is the amount of adsorbate (mg g^{-1}) at time t (min); and k_1 (min^{-1}) and k_2 ($g \cdot mg^{-1} \cdot min^{-1}$) are the rate constants for the pseudo first- and second-order adsorption, respectively.

Electrochemical characterizations

All electrochemical experiments were conducted in a conventional three-electrode electrochemical cell. The three-electrode electrochemical cell consisted of a calomel electrode reference electrode, a platinum counter electrode, and a modified glassy carbon working electrode. 0.2 mmol L^{-1} NaCl was selected as the electrolyte solution.

Preparation of modified working electrode

The Nafion solution with a mass fraction of 5 % was dissolved in a 1:1 isopropanol-water solution to prepare a Nafion solution with a mass fraction of 0.5 %. Then 2 mg of the material was added to 100 μL of 0.5 wt% solution. 5 μL of the suspension was dropped onto the surface of the disc electrode, which was air-dried for further use. Tafel polarization curve, open circuit potential (OCP), and electrochemical impedance spectroscopic (EIS) were performed by the CHI760E electrochemical workstation to elevate the electrochemical behavior of the materials. The electrochemical parameters are present as follow.

(1) Tafel polarization curve

The voltage range was -1.0V~ -0.5V (10 mV S^{-1}), and the corrosion potential was scanned twice.

(2) Electrochemical impedance spectroscopy (EIS)

EIS was carried out at the open-circuit voltage in the frequency range of 0.01 Hz to 100 kHz.

(3) Open circuit potential (OCP) curves

The OCP test time was 1500 s, sample interval 0.1 s. After the baseline was stable, the first solution was added at 300 s, and the second solution was added at 1100 s.

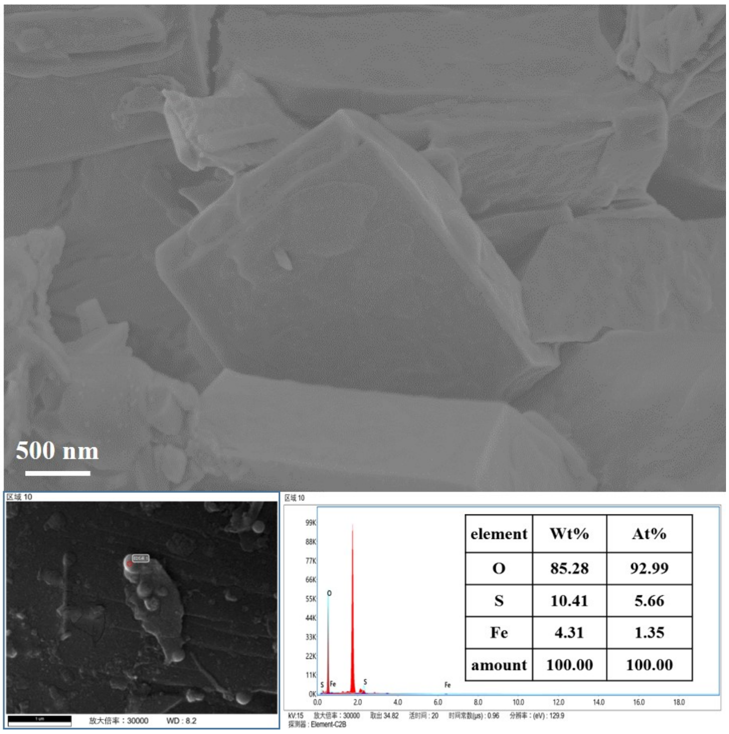

Fig. S1. SEM-EDS images of pristine FeS_2.

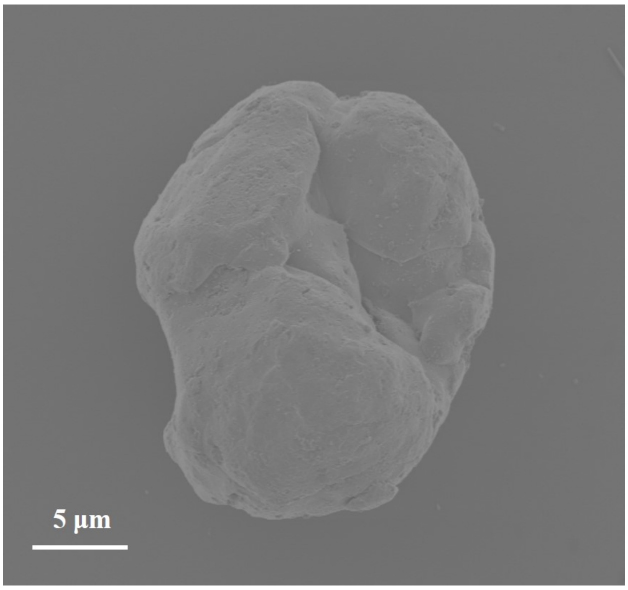

Fig. S2. SEM images of pristine ZVI.

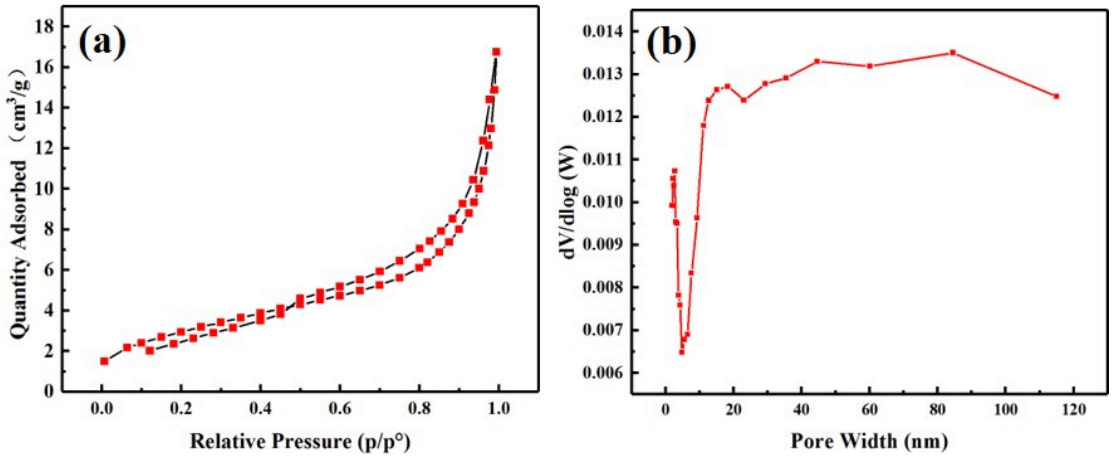

Fig. S3. (a) N_2 adsorption-desorption isotherm and (b) pore size distribution image of FeS_2/ZVI (molar ratio 9:1).

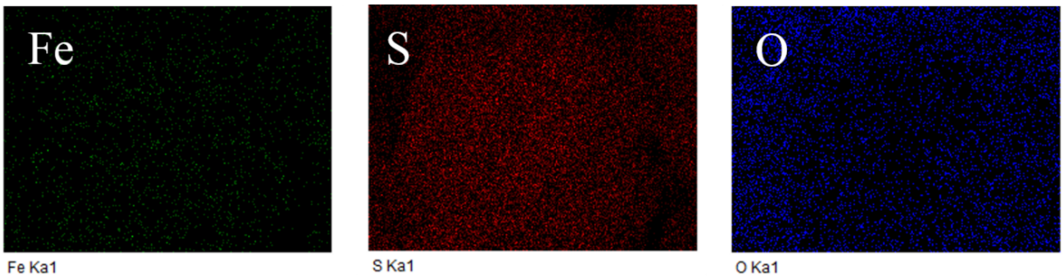

Fig. S4. EDS elemental mapping images of FeS_2/ZVI (molar ratio:9:1).

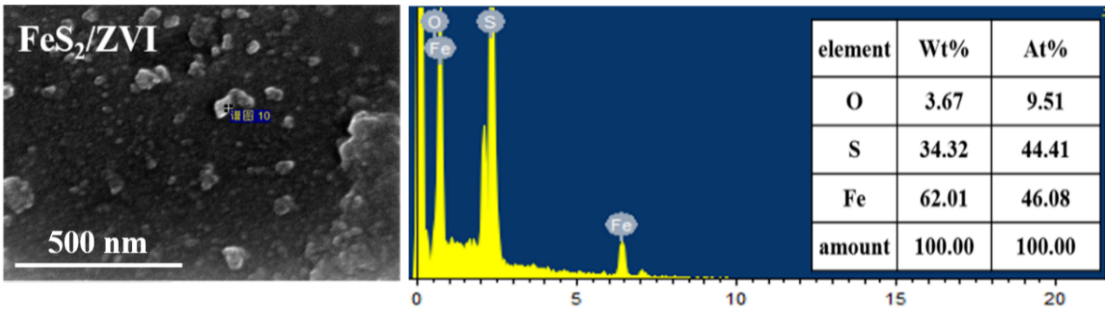

Fig. S5. SEM-EDS images of FeS_2/ZVI (molar ratio 9:1).

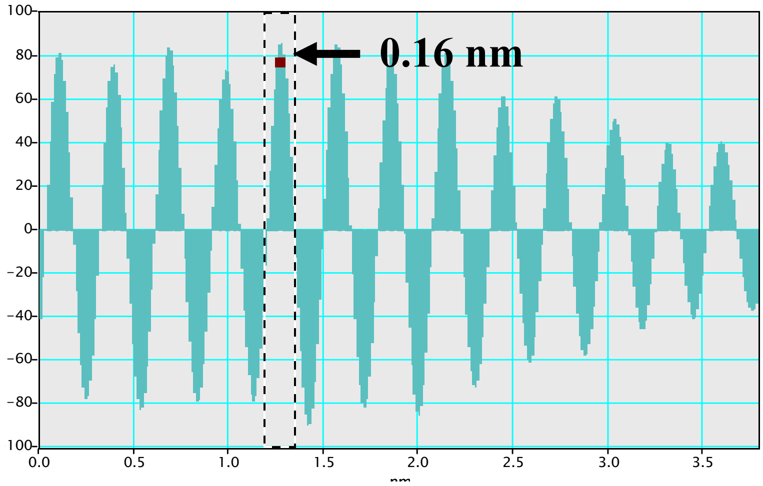

Fig. S6. D-spacing intensity profiles of the different regions of FeS_2/ZVI sample.

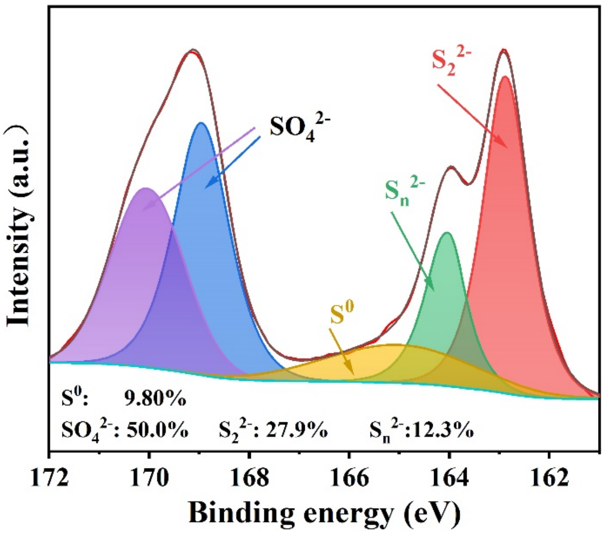

Fig. S7. S 2p XPS spectra of FeS_2/ZVI (molar ratio 9:1).

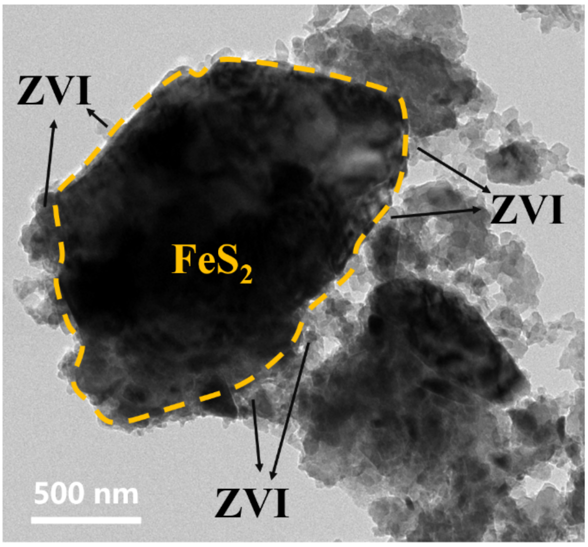

Fig. S8. TEM images of FeS_2/ZVI (molar ratio 9:1).

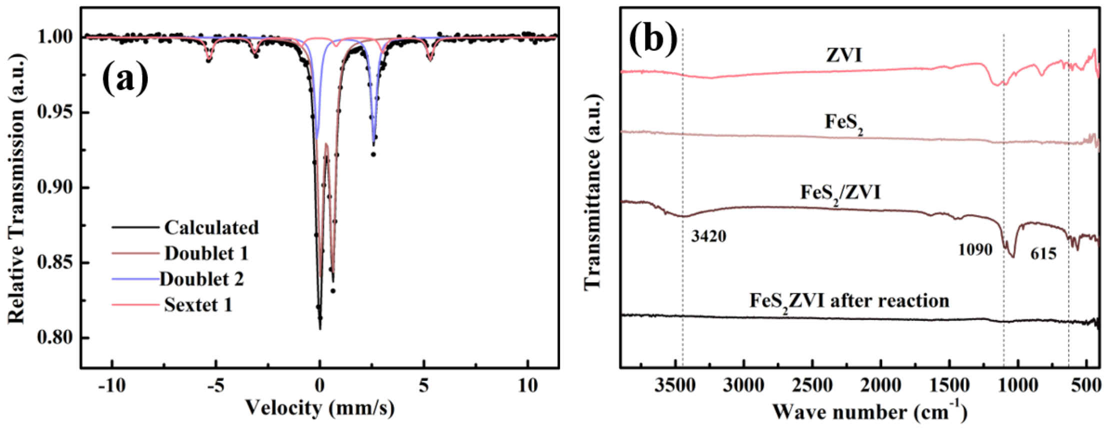

Fig. S9. (a) ^{57}Fe Mossbauer spectra of FeS_2/ZVI, (b) FTIR spectra of FeS_2, ZVI and FeS_2/ZVI before and after reaction with Cr(VI); (Particle dosage: 1 g L^{-1}, $[Cr(VI)]_0$ = 50.0 mg L^{-1}, pH_0 = 5.20, air atmosphere).

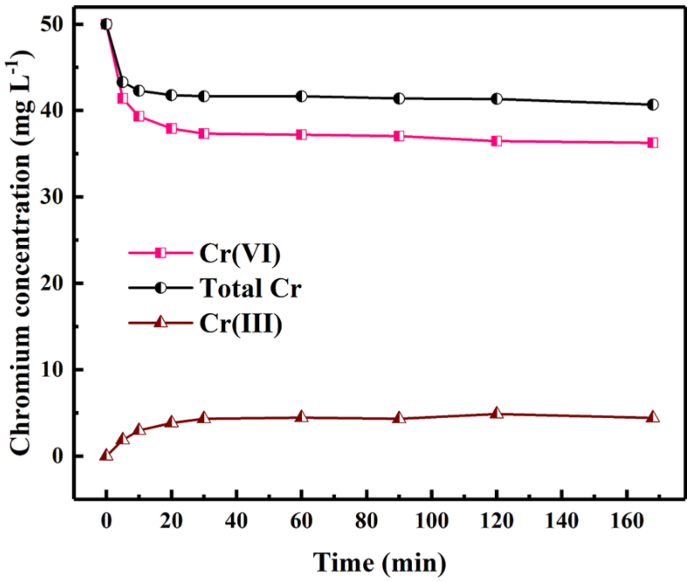

Fig. S10. The concentration of total Cr, Cr(VI) and Cr(III) during Cr(VI) removal by Mixed FeS_2-ZVI. (Particle dosage:1 g L^{-1}, $[Cr(VI)]_0$ = 50.0 mg L^{-1}, pH_0 = 5.20, air atmosphere).

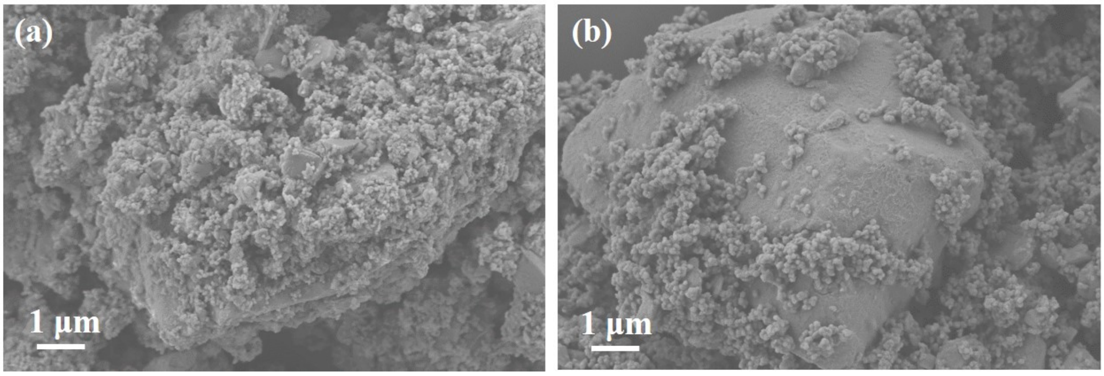

Fig. S11. SEM images of (a) mixed FeS_2-ZVI and (b) FeS_2/ZVI after Cr(VI) removal. (Particle dosage: 1 g L^{-1}, $[Cr(VI)]_0$ = 50.0 mg L^{-1}, pH_0 = 5.20, air atmosphere).

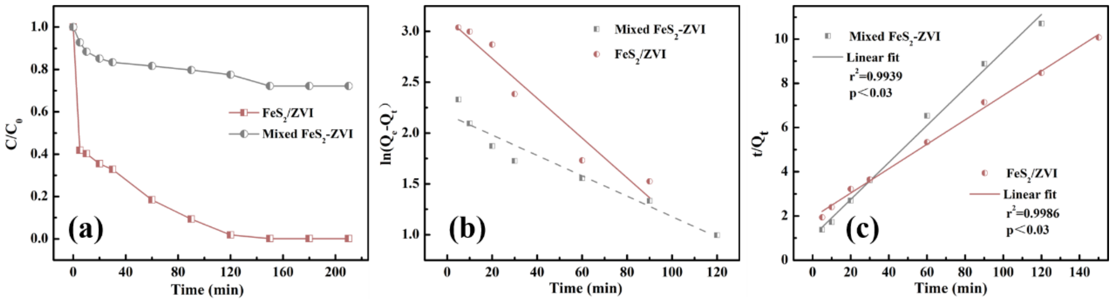

Fig. S12. (a) Cr(VI) removal by FeS_2/ZVI and mix FeS_2-ZVI, the fitting plots of (b) Pseudo first-order kinetic modeling and (c) pseudo-second-order by FeS_2/ZVI and mixed FeS_2-ZVI. (Particle dosage: 1 g L^{-1}, $[Cr(VI)]_0$ = 50.0 mg L^{-1}, pH_0 = 5.20, air atmosphere).

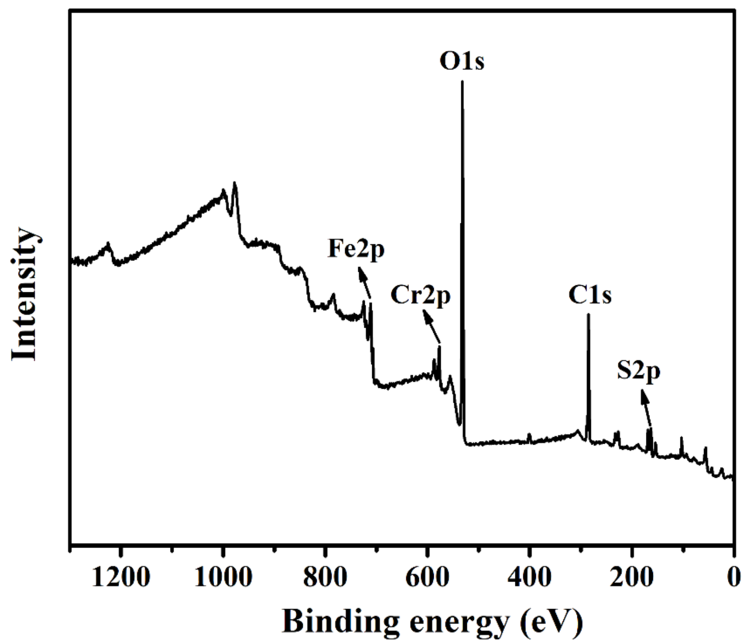

Fig. S13. XPS survey spectrum of FeS_2/ZVI after Cr(VI) removal.

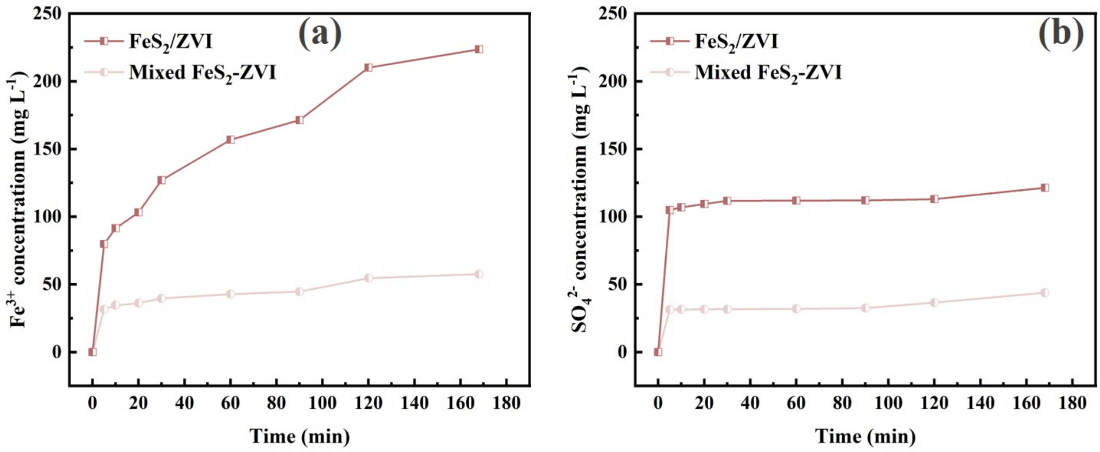

Fig. S14. The concentration of (a) Fe^{3+} and (b) SO_4^{2-} in the mixed FeS_2-ZVI system and FeS_2/ZVI system. (Particle dosage:1 g L^{-1}, $[Cr(VI)]_0$ = 50.0 mg L^{-1}, pH_0 = 5.20, air atmosphere).

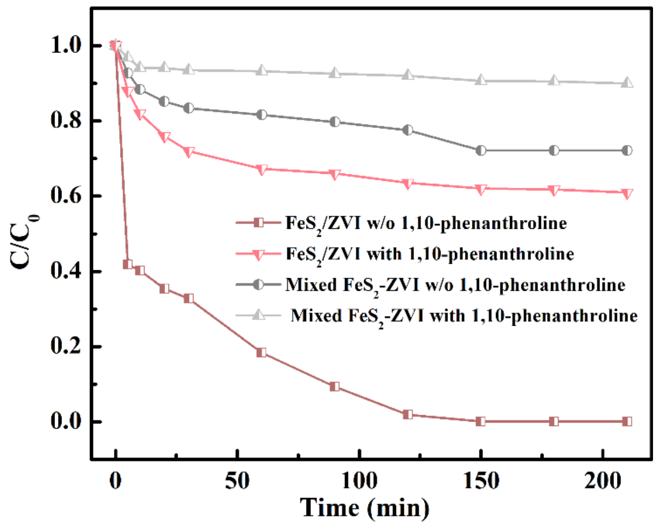

Fig. S15. (a) Cr(VI) removal by mixed FeS_2-ZVI and FeS_2/ZVI in the absence or presence of 1,10-phenanthroline. (Particle dosage: 1 g L^{-1}, $[Cr(VI)]_0$ = 50.0 mg L^{-1}, NaAc-HAc buffer solution, pH_0 = 3.93, air atmosphere).

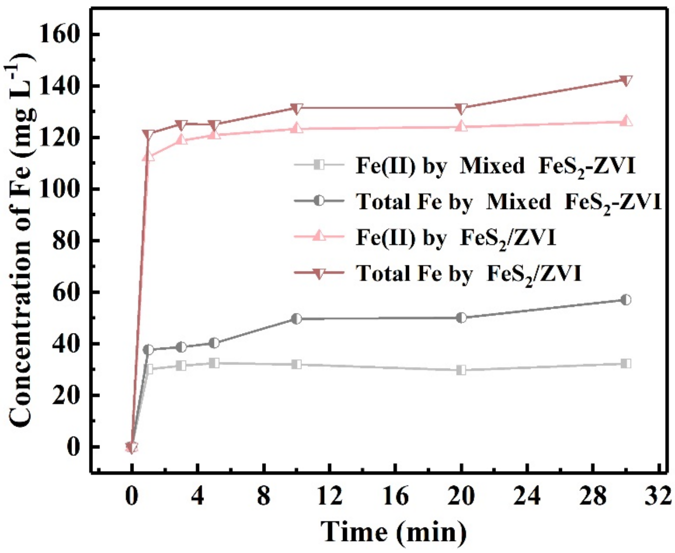

Fig. S16. Dissolution of Fe from mixed FeS_2-ZVI and FeS_2/ZVI in pure water system.

(Particle dosage: 1 g L^{-1}, air atmosphere).

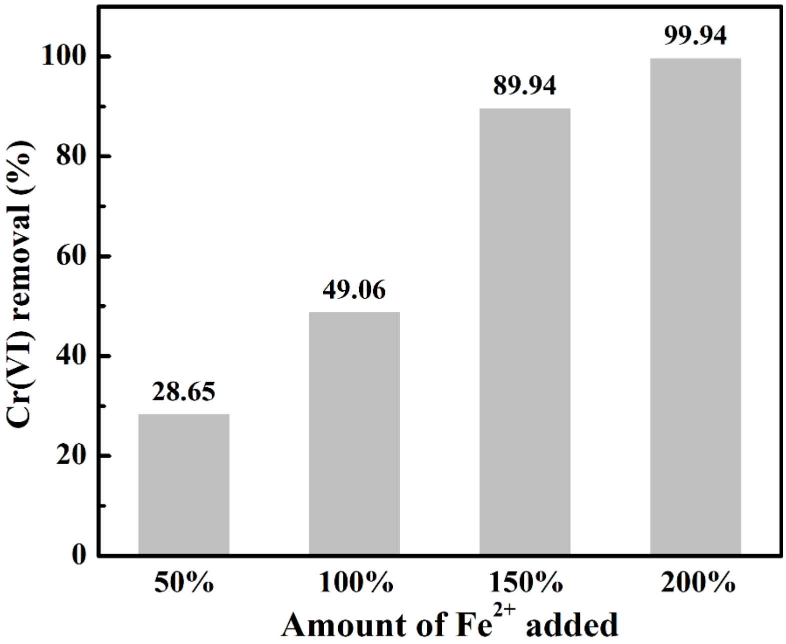

Fig. S17. Effect of different amount of Fe^{2+} added on Cr(VI) removal. ($[Cr(VI)]_0$ = 50.0 mg L^{-1}, pH_0 = 5.20, air atmosphere).

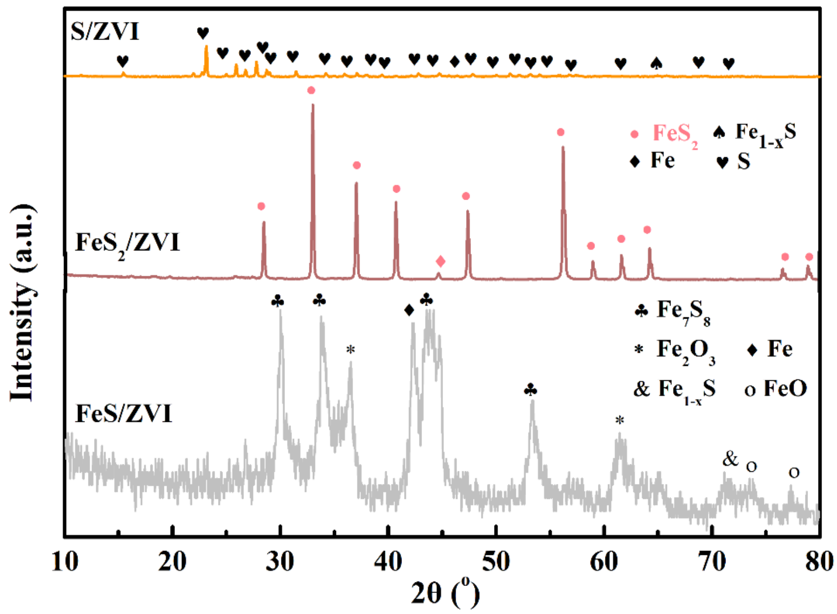

Fig. S18. XRD patterns of FeS_2/ZVI, FeS/ZVI and S/ZVI.

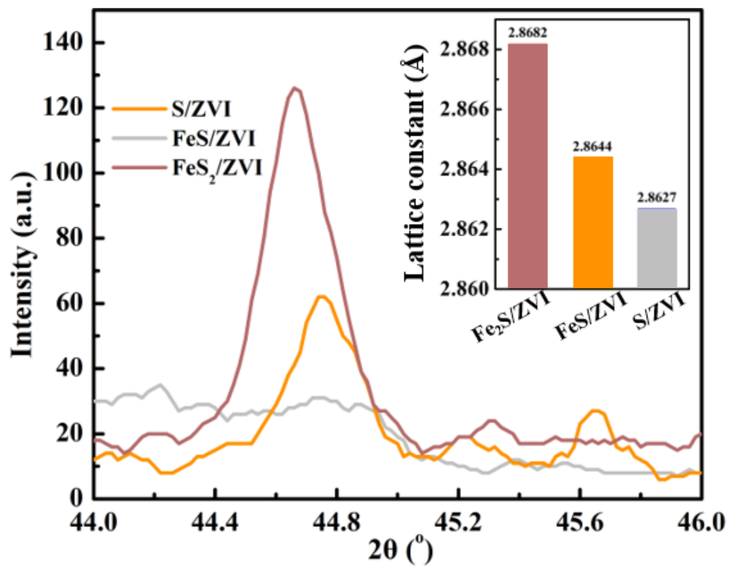

Fig. S19. Lattice constants of Fe BCC structure according to XRD Rietveld refinement

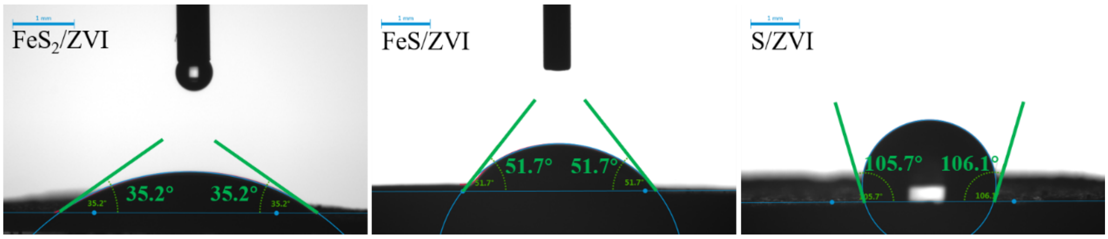

Fig. S20. Water contact angle images of FeS2/ZVI, FeS/ZVI, and S/ZVI.

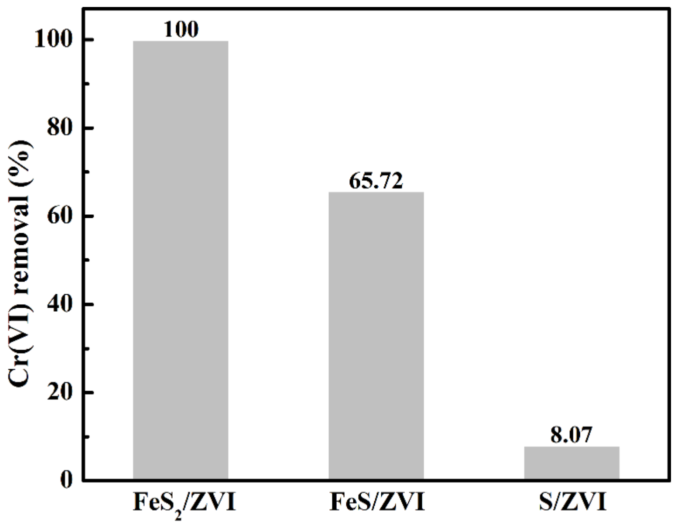

Fig. S21. The influence of S precursors on hydrophobicity and Cr(VI) removal. (Particle dosage: 1 g L^{-1}, $[Cr(VI)]_0$ = 50.0 mg L^{-1}, pH_0 = 5.20, air atmosphere).

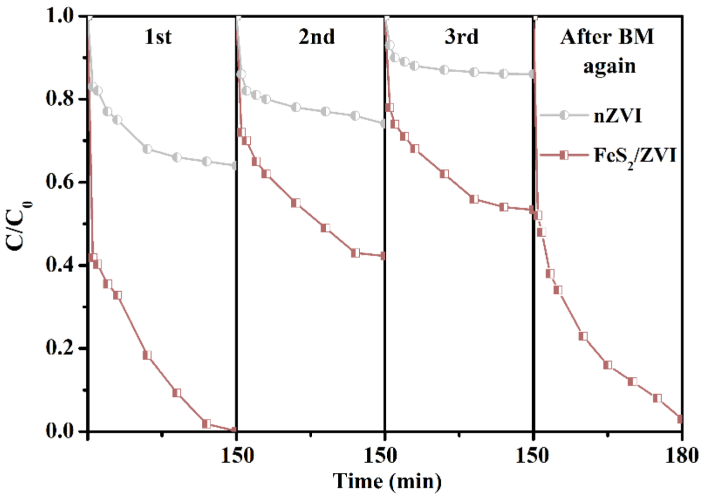

Fig. S22. The reusability of FeS_2/ZVI at initial pH 5.20 for Cr(VI) removal and rejuvenation of FeS_2/ZVI by BM again.

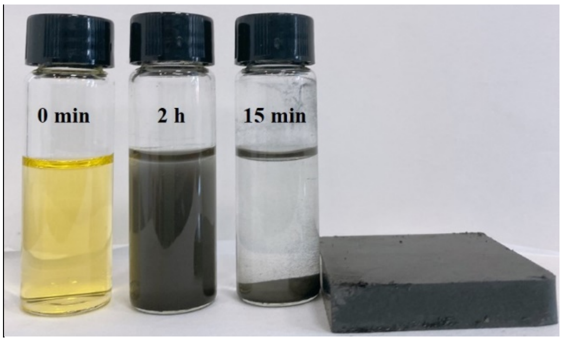

Fig. S23. Image of the magnetic separation after the Cr(VI) removal by FeS_2/ZVI.

Table S1. The ^{57}Fe Mossbauer parameters[a] of FeS_2/ZVI.

Component	H (KOe)	IS (mm s^{-1})	QS (mm s^{-1})	$\Gamma/2$ (mm s^{-1})	Fe%	Identified state of iron
Doublet 1		0.32	0.59	0.16	61.2	Fe^{2+}
Doublet 2		1.24	2.73	0.15	25.7	Fe^{3+}
Sextet 1	329.48	-0.02	0.05	0.16	13.1	Fe^{0}

[a]IS: isomer shift. QS: quadrupole splitting. H: hyperfine field. Γ/2: half-linear.

Table S2. Cr(VI) removal by FeS_2/ZVI at different FeS_2/ZVI molar ratio.

Molar ratio (FeS_2:ZVI)	9:1	10:1	11:1	10:0
Cr(VI) removal rate (%)	99.9	92.71	79.48	26.8

Table S3. Linear regression analysis of mixed FeS_2-ZVI and FeS_2/ZVI for the kinetics of Cr(VI) removal.

Parameter		FeS_2-ZVI	FeS_2/Fe^0
Pseudo first-order	k_1 (min^{-1})	0.01	0.0254
	Q_e (mg g^{-1})	13.92	49.93
	R^2	0.9355	0.9405
Pseudo second-order	k_2 (g mg^{-1} min^{-1})	0.006544	0.002137
	Q_e (mg g^{-1})	11.95	52.08
	R^2	0.9939	0.9986

Table S4. Intrinsic properties of FeS_2/ZVI (molar ratio 9:1).

Name	Content (mg g^{-1})		Specific surface area (m^2 g^{-1})	S speciation (%)				Lattice constant (Å)
	Fe	S		SO_4^{2-}	S^0	S_n^{2-}	S_2^{2-}	
FeS_2/ZVI	770	175	10.9	50.0	9.80	12.3	27.9	2.861